Research Article
Molecular and Cell Biology

JOURNAL
OF HEPATOLOGY

Reactive cholangiocytes differentiate into proliferative hepatocytes with efficient DNA repair in mice with chronic liver injury

Graphical abstract

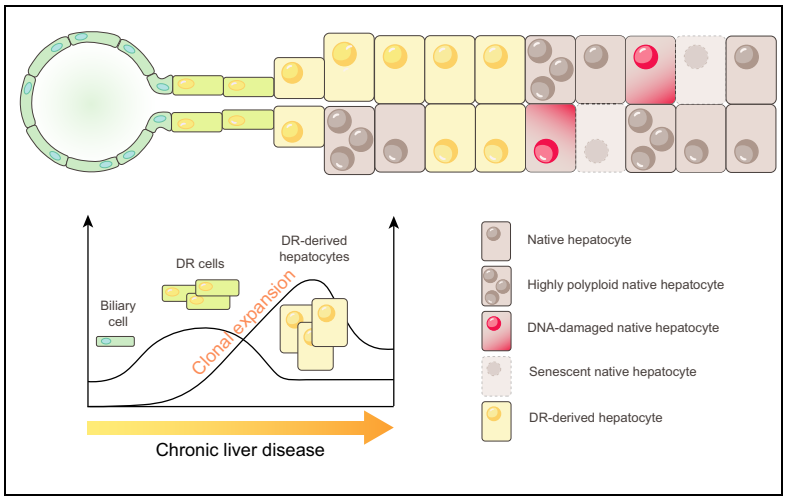

Highlights

- During chronic injury, native hepatocytes become damaged, replicatively senescent and accumulate DNA damage.
- New hepatocytes with specific characteristics of "undamaged and young hepatocytes emerge and undergo clonal expansion.
- Our cell tracing studies suggest that these new hepatocytes derive from reactive cholangiocytes.

Authors

Rita Manco, Laure-Alix Clerbaux, Stefaan Verhulst, ..., Leo van Grunsven, Chantal Desdouets, Isabelle Leclercq

Correspondence

isabelle.leclercq@uclouvain.be
(I. Leclercq)

Lay summary

During chronic liver disease, while native hepatocytes are exhausted and genetically unstable, a subset of cholangiocytes clonally expand to differentiate into young, functional and robust hepatocytes. This cholangiocyte cell population is a promising target for regenerative therapies in patients with chronic liver insufficiency.

http://dx.doi.org/10.1016/j.jhep.2019.02.003
 J. Hepatol. 2019, 70, 1180–1191

Research Article
Molecular and Cell Biology

JOURNAL OF HEPATOLOGY

Reactive cholangiocytes differentiate into proliferative hepatocytes with efficient DNA repair in mice with chronic liver injury

Rita Manco[1], Laure-Alix Clerbaux[1], Stefaan Verhulst[2], Myriam Bou Nader[3,4,5], Christine Sempoux[6], Jerome Ambroise[7], Bertrand Bearzatto[7], Jean Luc Gala[7], Yves Horsmans[1,8], Leo van Grunsven[2], Chantal Desdouets[3,4,5], Isabelle Leclercq[1,*]

[1]*Laboratory of Hepato-gastroenterology, Institut de Recherche Expérimentale et Clinique, Université catholique de Louvain, Brussels, Belgium;* [2]*Liver Cell Biology Laboratory, Vrije Universiteit Brussels (VUB), Brussels, Belgium;* [3]*Inserm, U1016, Institut Cochin, Paris, France;* [4]*CNRS, UMR 8104, Paris, France;* [5]*Université Paris Descartes, Sorbonne Paris Cité, Paris, France;* [6]*Institute of Pathology, Centre Hospitalier Universitaire Vaudois, Lausanne, Switzerland;* [7]*Centre de Technologies Moléculaires Appliquées, Institut de Recherche Expérimentale et Clinique, Université catholique de Louvain, Brussels, Belgium;* [8]*Hepato-gastroenterology Unit, Cliniques Universitaires Saint-Luc, Brussels, Belgium*

See Editorial, pages 1051–1053

Background & Aim: Chronic liver diseases are characterized by expansion of the small immature cholangiocytes – a mechanism named ductular reaction (DR) – which have the capacity to differentiate into hepatocytes. We investigated the kinetics of this differentiation, as well as analyzing several important features of the newly formed hepatocytes, such as functional maturity, clonal expansion and resistance to stress in mice with long-term liver damage.

Methods: We tracked cholangiocytes using osteopontin-iCreER^{T2} and hepatocytes with AAV8-TBG-Cre. Mice received carbon tetrachloride (CCl_4) for >24 weeks to induce chronic liver injury. Livers were collected for the analysis of reporter proteins, cell proliferation and death, DNA damage, and nuclear ploidy; hepatocytes were also isolated for RNA sequencing.

Results: During liver injury we observed a transient DR and the differentiation of DR cells into hepatocytes as clones that expanded to occupy 12% of the liver parenchyma by week 8. By lineage tracing, we confirmed that these new hepatocytes derived from cholangiocytes but not from native hepatocytes. They had all the features of mature functional hepatocytes. In contrast to the exhausted native hepatocytes, these newly formed hepatocytes had higher proliferative capability, less apoptosis, a lower proportion of highly polyploid nuclei and were better at eliminating DNA damage.

Conclusions: In chronic liver injury, DR cells differentiate into stress-resistant hepatocytes that repopulate the liver. The process might account for the observed parenchymal reconstitution in livers of patients with advanced-stage hepatitis and could be a target for regenerative purposes.

Lay summary: During chronic liver disease, while native hepatocytes are exhausted and genetically unstable, a subset of cholangiocytes clonally expand to differentiate into young, functional and robust hepatocytes. This cholangiocyte cell population is a promising target for regenerative therapies in patients with chronic liver insufficiency.

Introduction

Persistent injury of the hepatic tissue leads to fibrosis, which eventually evolves to cirrhosis, the end-stage of any chronic liver diseases. Cirrhosis is characterized by distortion of hepatic architecture, regenerative nodules and hepatocyte dysfunction and is associated with life-threatening complications such as hepatocellular insufficiency and hepatocellular carcinoma (HCC).[1] Liver cirrhosis is estimated to cause around 170,000 deaths annually.[2] So far, liver transplantation represents the only curative therapeutic solution for many chronic liver diseases.

In chronic liver diseases, extension of the fibrotic scars correlates with the presence of "ductular reaction" (DR).[3,4] This term refers to proliferation of small immature cholangiocytes, located at the most proximal branches of the biliary tree.[5,6] DR cells (also referred to as oval cells or liver progenitor cells) express hepatocyte (CK8, CK18) and cholangiocyte (OV-6, CK7, CK19)[7–9] markers and have the potential to differentiate into either of these 2 liver epithelial lineages.[10] Studies on human chronic liver diseases, including chronic viral hepatitis, autoimmune hepatitis and cirrhotic alcoholic or non-alcoholic fatty liver diseases, have highlighted substantial DR and the emergence of cells intermediate in size and immunophenotype between DR cells and hepatocytes.[3,11] Several studies report that such intermediate cells represent more than half of the hepatocyte pool in the cirrhotic liver.[8,9,12] A morphological continuum between DR, intermediate cells and hepatocytes may be interpreted as a gradual differentiation of DR in hepatocytes or as a de-differentiation of hepatocytes with acquisition of biliary traits (metaplasia). This conundrum is hard to resolve by the observation of human material. For this reason, several (inducible) lineage tracing mouse strains tagging either cholangiocytes/DR cells or hepatocytes have been used in the last decade in attempt to unravel the origin, the dynamics and the fate of DR cells in various dietary, chemical or genetic rodent

Keywords: Lineage tracing; Mouse model; Regeneration; Cell therapy.
Received 9 October 2018; received in revised form 1 February 2019; accepted 4 February 2019; available online 20 February 2019
* Corresponding author. Address: GAEN Laboratory, Avenue Mounier 53, B1.52.01, 1200 Brussels, Belgium. Tel.: +32 2764 5273.
E-mail address: isabelle.leclercq@uclouvain.be (I. Leclercq).

models of liver injury. The results of these studies remain conflicting. Studies by us and other authors, in which the fate of DR cells or hepatocytes was followed after hepatocellular injury caused by a choline-deficient and ethionine-supplemented (CDE) diet, support the *in vivo* capability of DR to differentiate into hepatocytes, although in discrete proportions (<2.5%).[13–15] Furthermore, DR cells isolated from CDE livers largely underwent hepatocyte differentiation when transplanted *in vivo* into a compromised liver, with an improvement of both liver architecture and function.[16] In zebrafish the biliary compartment is also capable of generating functional hepatocytes.[17] On the other hand, studies using the 3,5-diethoxycarbonyl-1,4-dihydro collidine (DDC) diet as model of cholangiocytic injury failed to demonstrate a contribution of DR to the hepatocyte pool[18,19] and other works even support a de-differentiation of traced hepatocytes into biliary-like cells.[20–22] Taken together such inconsistent data indicate that the involvement of DR cells in regeneration is conditioned by the epithelial compartment undergoing damage and is thus disease-specific; while considerable discrepancies between models and observations in human material may stem from fundamental differences in severity and chronicity of injury. Here, we aimed to analyze DR and its contribution to regeneration in a model replicating chronicity, severity and fibrotic progression seen in chronic hepatitis in humans.

Impaired hepatocyte proliferative capacity is the essential requirement for DR.[23] Recently, the capacity of the DR cells to maintain the liver parenchyma was demonstrated using genetic approaches to induce hepatocyte replicative senescence or growth arrest: i) deletion of *Mdm2*[16] to provoke p53-mediated senescence in all the hepatocytes; ii) deletion of β1-integrin[24] to inhibit hepatic growth factor signaling thereby precluding hepatocyte replication, or of β-catenin directly in the hepatocytes to impair their proliferation;[25] iii) the overexpression of p21 in conjunction with induction of injury using a DDC diet, a methionine-choline deficient diet and thioacetamide (TAA).[24] Such genetic models artificially cause subacute hepatocyte failure, as opposed to progressive lesions occurring during chronic liver injury. Thus, Deng *et al.* demonstrated the capability of DR cells to differentiate into hepatocytes in a long-term injury model (up to 52 weeks) using the toxic agent TAA.[26] However, the kinetics of the response to the injury, as well as several features of the DR-derived hepatocytes, such as level of maturation, clonal expansion and resistance to stress remain unanswered.

Here, we used a model of chronic liver injury mimicking the evolution and severity of chronic human diseases to follow the fate of DR cells, evaluating their contribution to the pool of hepatocytes and characterizing the newly formed hepatocytes. We show that DR emerges from clonal expansion of cholangiocytes; DR cells then undergo hepatocyte differentiation and clonal proliferation. Hepatocyte lineage tracing studies confirmed that these emerging cells are not of hepatocyte origin.

The mature and newly formed functional hepatocytes have a survival, proliferative and DNA repair advantage that favors their amplification over native hepatocytes (*i.e.* those arising from division of pre-existent hepatocytes).

Materials and methods

Animal models

To follow the fate of biliary/DR cells we used Osteopontin-iCreER^{T2} (OPN-Cre) mice crossed with Rosa26R^{YFP}, Rosa26R$^{mT/mG}$ or Rosa26R^{Confetti}.[27–29] To achieve *Cre-LoxP* recombination, tamoxifen (T5648; Sigma) at a concentration of 30 mg/ml corn oil was injected intraperitoneally at 100 mg/kg of bodyweight for 2 consecutive days on 21 and 23 days old OPN-Cre; Rosa26R^{YFP} and OPN-Cre;Rosa26R$^{mT/mG}$ mice or at 175 mg/kg of bodyweight for 5 days to ≥ 40 g OPN-Cre; Rosa26R^{Confetti} mice.[30] To genetically label the hepatocytes, AAV8-TBG-Cre adenovirus was injected intravenously at a concentration of 7, 5x10^{11} gc/mouse in Rosa26R^{YFP} or Rosa26R$^{mT/mG}$ reporter mice.[31] We used yellow fluorescent protein (YFP) immunohistochemistry (IHC) or direct observation under the fluorescence microscope to analyze tagged cells, respectively (see Supplementary Information). One month after tamoxifen treatment (to ensure complete tamoxifen wash-out) chronic liver injury was induced by repeated intraperitoneal injection of carbon tetrachloride (CCl_4) 3 times per week for 4, 6, 8, 16 and 24 weeks. The starting dose of CCl_4 was 500 µl/kg, with dose increase up to 800 µl/kg when animals gained weight. Livers were analyzed 72 h after the last CCl_4 injections or after a 2- or 4-week CCl_4-free recovery period. Transgenic mice that did not receive tamoxifen were used as controls. The size of the groups is specified in the figure legends.

Mice were housed at 4–5/cage, maintained at a constant temperature of 22 °C, exposed at all times to a 12 h light/12 h dark cycle and had access to food and water *ad libitum*. Animal care was provided in accordance with the guidelines for humane care for laboratory animals in accordance with European regulations and in conformity with ARRIVE guidelines. The study protocol was approved by the university ethics committee for the use of experimental animals (2012/MD/UCL/026 and 2016/UCL/MD/003).

FACS sorting analysis

Livers from control OPN-Cre;Rosa26R$^{mT/mG}$ mice were dissociated using pronase and collagenase to obtain a single cell suspension.[32] Two centrifugations of 50 g were performed to separate the non-parenchymal fraction from the hepatocytes. We blocked the non-parenchymal fraction using bovine serum albumin for 10 min and incubated cells with the indicated antibodies for 15 min. After adding propidium iodide we used a FACSAriaII (BD) to isolate liver sinusoidal endothelial cells ($CD32^+F4/80^-$ UV^-PI^-), macrophages ($F4/80^+CD32^-UV^-PI^-$), hepatic stellate cells ($UV^+F4/80^-CD32^-PI^-$) and biliary epithelial cells ($EpCAM^+UV^-CD45^-PI^-$). Hepatocytes were resuspended in PBS and immediately sorted. In each population cells were analysed for tdTomato (red) and mGFP (green) fluorescence.

For the isolation of hepatocytes and RNA sequencing (RNA-seq), livers from tamoxifen-injected untreated and CCl_4 treated OPN-Cre;Rosa26R$^{mT/mG}$ mice were digested using a 2-step collagenase method. Solutions were perfused through the portal vein. Two centrifugations of 50 g were performed to separate the non-parenchymal cells from the hepatocytes. The resulting hepatocyte populations were filtered through a 100 µm filter and resuspended in 2 mM EDTA + 1% FBS solution and sorted by a FACSAriaIII (BD) according to the presence of mTomato and mGFP fluorescence. Dead cells were excluded by ToPro3 staining. Sorted cells where lysed and the RNA was extracted using Qiagen RNeasy Mini kit (Promega) and processed for RNAseq. Hepatocytes were also isolated from control mice, 4 weeks and 6 weeks CCl_4-treated wild-type mice using the 2-step collagenase method. The resulting hepatocytes were cul-

tured on 6-well collagen-coated dishes for 24 h in DMEM/F12 + 10% FBS and used for immunofluorescence detection.

Polyploidy analysis

Immunostained liver sections (β-catenin/YFP/Hoechst) were imaged with a nanozoomer 2.0, Hamamatsu fluorescent microscope associated with image management software NDP view. For ploidy analysis, Hoechst labelling was used to recognize hepatocytes nuclei with a roundness >0.8. Nuclear area was detected automatically by a specific macro developed with ImageJ software (pixels ranging from 200 to 2,500 px2). For each animal analyzed, more than 10,000 nuclei were counted.

IHC score of liver tumors

Consecutive liver sections stained for CK19, glutamine synthetase (GS encoded by *Glul*), β-catenin and Ki67 were scored by the expert pathologist Dr. Christine Sempoux. Nodules with a diameter >1.5 mm were selected and evaluated as follow: GS was classified as normal (0) when expressed around the central vein or aberrant (1) if the expression was diffuse in the nodule or completely lost; β-catenin was evaluated as normal (1), cytoplasmatic (2) or cytoplasmatic/nuclear (3); Ki67 was classified as less than 10% (1), 10–25% (2) or more than 25% (3) level. None of the nodules expressed CK19.

Statistical analysis

Data are presented as mean value ± SEM. Statistical analyses were performed using a paired 2-tailed Student *t* test, a 1-way ANOVA followed by Bonferroni's *post hoc*, a Kolmogorov-Smirnov test for rank as appropriate using Graph Pad Prism 5 software. Differences were considered significant at values of $p < 0.05$.

Additional information on methods (carcinogenetic animal model, qPCR analysis, immunohistochemistry, RNAseq) is provided in the supplementary information.

Results

DR cells differentiate into hepatocytes, contributing significantly to the liver parenchyma

Mice were repeatedly injected with CCl_4 for up to 16 weeks (Fig. 1A) to induce repeated cycles of central necrosis and wound healing, leading to progressive fibrosis. Sirius red

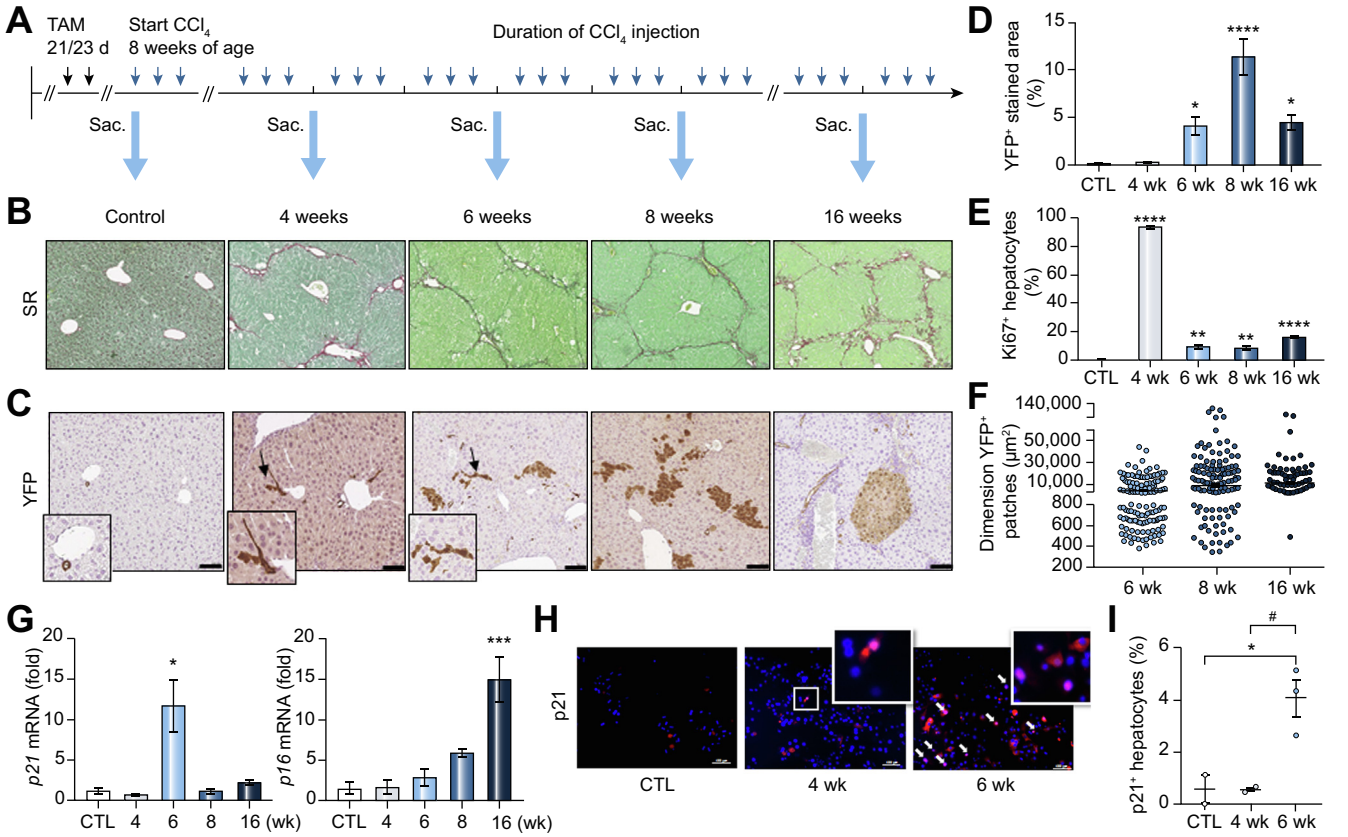

Fig. 1. DR cells significantly contribute to the hepatocyte pool during chronic liver injury. (A) Schematic representation of the experimental design. (B) Liver section obtained from OPN-iCreER^{T2};Rosa26R^{YFP} mice treated for 0 (n = 6), 4 (n = 2), 6 (n = 5), 8 (n = 4) and 16 (n = 4) weeks with CCl_4, stained with Sirius red for collagen (Scale bar: 100 µm). (C) Representative YFP immunohistochemistry on liver sections from OPN-iCreER^{T2};Rosa26R^{YFP} controls or mice treated with CCl_4 for 4, 6, 8 and 16 weeks. (Scale bar: 100 µm) (D) Morphometric quantification of the YFP positive area; (E) Ki67$^+$ hepatocyte quantification in control and treated mice. Values are expressed as means of percentage ± SEM; (F) Size of the YFP$^+$ patches from the liver sections of OPN-iCreER^{T2};Rosa26R^{YFP} mice treated with CCl_4 for 6, 8 and 16 weeks. (G) Genes involved in senescence and cell cycle arrest pathways were determined by RT-qPCR. (H) Representative images of isolated hepatocytes stained for p21. (Scale bar: 100 µm) (I) quantification of the p21+ hepatocytes. Values are expressed as mean ± SEM relatively to controls. *$p < 0.05$; ***$p < 0.001$; ****$p < 0.0001$ by 1-way ANOVA. CCl_4, carbon tetrachloride; DR, ductular reaction; RT-qPCR, reverse transcription quantitative PCR; YFP, yellow fluorescence protein.

staining revealed central bridging fibrosis after 4 weeks, extension and thickening of fibrotic bundles progressively increased with time (Fig. 1B).

During the injury, we followed the fate of biliary/DR cells using tamoxifen-inducible osteopontin-i*CreER*^{T2} (OPN-Cre) mice crossed with Rosa26R^{YFP} or with Rosa26R$^{mT/mG}$ reporter mice to label biliary cells. Activation of the OPN promoter in cholangiocytes drives the expression of the inducible Cre recombinase. Tamoxifen binds the mutated estrogen receptor ER^{T2} and allows the activation and the translocation of the Cre recombinase into the nucleus. Nuclear Cre recombinase was only found in biliary OPN^{+} cells in tamoxifen-injected OPN-Cre;Rosa26R^{YFP} mice but not in mice that did not receive tamoxifen (Fig. S1A). Recombination of the *Rosa26R* locus ensued and, according to the reporter strain, caused permanent expression of YFP in >85% of the cells of the biliary compartment or switched the expression of mTomato to that of mGFP in OPN-expressing cells with a 60% efficiency (Fig. S1B-D). No YFP^{+} or mGFP^{+} cells have been observed in livers harvested from tamoxifen-free OPN-Cre;Rosa26R^{YFP} or OPN-Cre;Rosa26R$^{mT/mG}$ mice, respectively (Fig. S1B; not shown). As reported by us[13,31] and others[33] and verified here again by cell sorting in tamoxifen-treated OPN-Cre;Rosa26R$^{mT/mG}$ mice (Fig. S1C and Fig. S2), upon tamoxifen injection, reporter gene expression is restricted to the biliary compartment and does not occur in hepatocytes, stellate cells, liver sinusoidal endothelial cells or Kupffer cells.

With this system, in the course of CCl_4 treatment, any YFP^{+} hepatocyte would be of biliary origin. After 4 weeks of tamoxifen wash-out, mice were treated with CCl_4. After 4 weeks of CCl_4, rare YFP^{+} hepatocyte-like cells were observed in the vicinity of DR (Fig. 1C). As the duration of liver insult increased, the number of YFP^{+} hepatocytes increased to reach a maximum at the 8-week time-point, such that 12% of the liver parenchyma was occupied by DR-derived hepatocytes (Fig. 1C-D). By contrast, in tamoxifen-free OPN-Cre;Rosa26R^{YFP} mice, no YFP^{+} cells and in particular no YFP^{+} hepatocytes where found in the course of CCl_4 treatment (Fig. S3). Thus, DR cells give rise to hepatocyte-like cells during chronic wound healing, supporting results shown in previous study.[26]

The emergence of YFP^{+} hepatocytes-like cells after 6 weeks of CCl_4 coincided with a marked drop in proliferative activity of native hepatocytes as assessed by Ki67 index (Fig. 1E and Fig. S4), as well as with an increased expression of p16 and p21 senescence markers (Fig. 1G). To confirm senescence in hepatocytes, we isolated and cultured fresh hepatocytes from controls and from mice treated with CCl_4 for 4 weeks and 6 weeks. Senescence-associated β-galactosidase activity (not shown) and P21 expression (Fig. 1H-I) were readily seen in isolated hepatocytes from 6-week CCl_4 samples but not from controls or 4-week CCl_4 livers. Senescence persists in the liver for the duration of the CCl_4 insult, as demonstrated by progressive increase in p21 protein in whole liver extracts (Fig. S5). The YFP^{+} hepatocytes formed patches, whose size increased with disease progression (Fig. 1C-F). After 6 weeks of CCl_4, a majority (>70%) of clusters were composed of 2–3 YFP^{+} hepatocyte-like cells. Over time, the proportion of small clusters declined while the

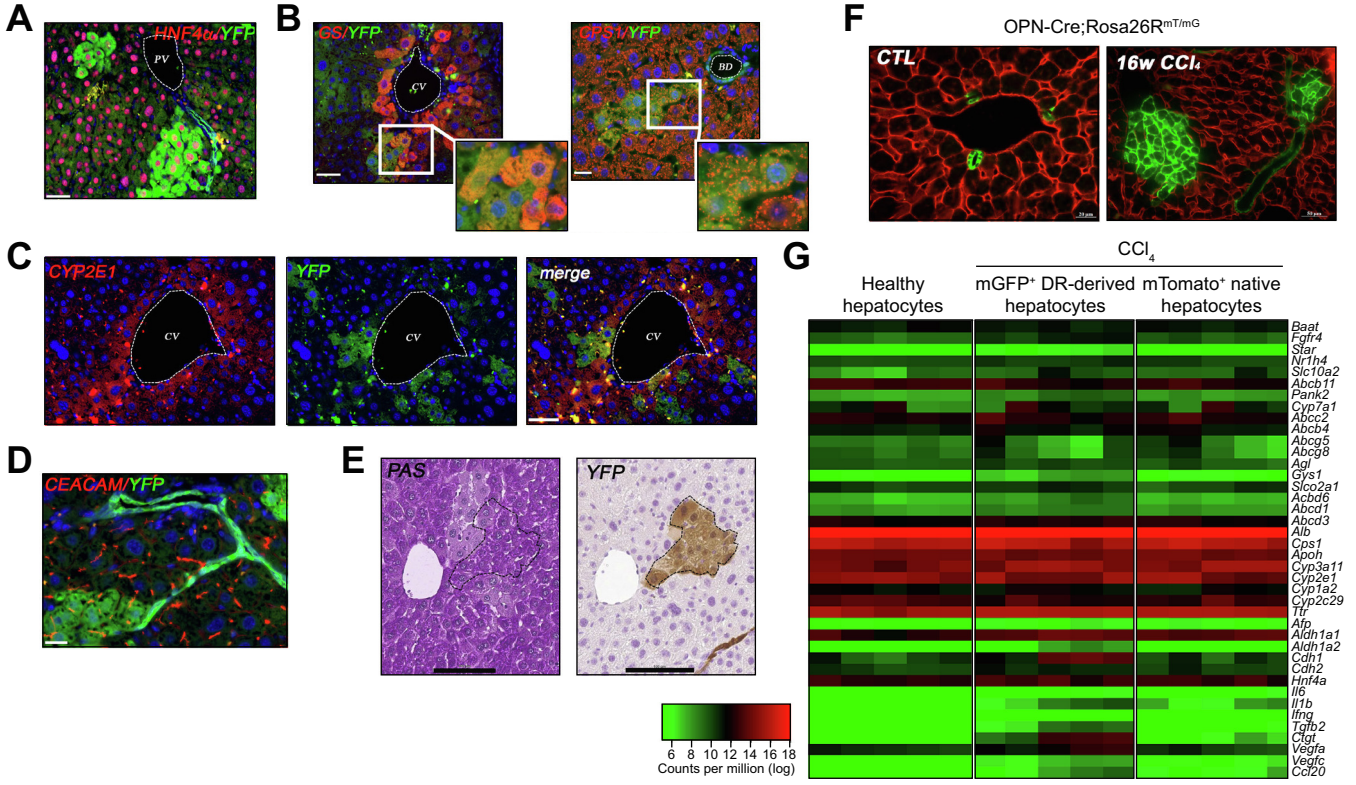

Fig. 2. DR-derived hepatocytes are fully mature hepatocytes. Representative pictures of liver sections from tamoxifen-injected-OPN-iCreER^{T2};Rosa26R^{YFP} animals treated with CCl_4 during 8 weeks stained for (A) HNF4α (red)/ YFP (green), (B) GS (red)/YFP (green) and CPS1 (red)/YFP (green), (C) CYP2E1 (red)/YFP (green), (D) CEACAM1 (red)/YFP (green) (scale bars: 50 μm). (E) Consecutive sections stained for glycogen (periodic acid-Schiff (PAS) and YFP (brown) (Scale bar: 100 μm). (F) Representative pictures of liver sections from tamoxifen-injected OPN-iCreER^{T2};Rosa26R$^{mT/mG}$ mice control (Scale bar: 20 μm) and treated for 16 weeks with CCl_4 (Scale bar: 50 μm) (G) RNA sequencing data generated heatmap displays similar expression of mature and functional hepatocytic genes (n = 5/group). CCl_4, carbon tetrachloride; CV, central vein; DR, ductular reaction; YFP, yellow fluorescence protein.

proportion of larger ones increased (Fig. 1F). The YFP$^+$ hepatocytes were HNF4α positive (Fig. 2A) and expressed hepatospecific liver enzymes according to their lobular location, such as expression of GS and CYP2E1 when pericentral or of CPS1 when periportal (Fig. 2B-C). Ceacam1 staining confirmed that YFP$^+$ hepatocytes were polarized and formed bile canaliculi with adjacent hepatocytes whether YFP$^+$ or YFP$^-$ (Fig. 2D). Also, YFP$^+$ cells stored glycogen similarly to native YFP$^-$ hepatocytes (Fig. 2E). However, they did not express biliary markers, such as CK19, the antigen EpCAM or the cholangiocyte factor HNF1β (Fig. S6). We isolated native (mTomato$^+$) and DR-derived (mGFP$^+$) hepatocytes from OPN-Cre;Rosa26R$^{mT/mG}$ after 16 weeks of CCl_4 (Fig. 2F; Fig. S7) and compared their transcriptome by RNAseq analysis. Healthy mTomato$^+$ hepatocytes from untreated OPN-Cre;Rosa26R$^{mT/mG}$ served as controls (Fig. 2F). In the 3 populations, there was a similarly high count of hepatospecific genes such as albumin (*Alb*), Transthyretin (*Ttr*) and *Cyp7a1* (Fig. 2G). They also had similar expression of *Cyp2E1* and GS (Fig. S8).

To confirm that the new hepatocytes do not come from the division of pre-existing hepatocytes in the CCl_4 injury model,[34] we performed an independent mirror experiment in which hepatocyte fate was analysed. Injection of AAV8-TBG-Cre adeno-associated virus to Rosa26R^{YFP} mice induced YFP expression in nearly 100% of hepatocytes and zero cholangiocytes or non-parenchymal cells (Fig. S9). Following chronic CCl_4 injections (Fig. S10A), patches of unlabelled HNF4α$^+$ and CK19$^-$ hepatocytes emerged in the liver (Fig. 3A-B). Their size grew with duration of injury comparably to the patches of DR-derived hepatocyte traces using the OPN-CreER^{T2};Rosa26^{YFP} system (Fig. 3C). This confirms the emergence of clusters of hepatocytes not derived from division of pre-existing labelled hepatocytes.

Long-term CCl_4 induces a discrete and transient DR

We then evaluated the kinetics of the DR response. CK19$^+$ bile ducts, normal in number and in morphology, were present in controls as well as diseased livers. After 4 and 6 weeks of CCl_4, in addition to normal bile ducts, discrete DR appeared as strings of CK19$^+$ small cells irradiating into the parenchymal lobule from the portal tract (Fig. 4A,B). Interestingly, in livers treated for longer duration (8–16 weeks), although the DR-derived hepatocytes increased in number (Fig. 1C,D), CK19$^+$ cells were limited to bile ducts and no DR was observed (Fig. 4A,B). The expression of Sox9 (a biliary transcription factor),[35] Fn14 (a cell membrane receptor that transduces mitogenic signals to DR cells),[36] Epcam and NCAM (cell adhesion molecules highly expressed in DR),[37] all genes expressed explicitly in cholangiocytes but not in hepatocytes (Fig. S11), confirmed the transient activation of a DR during the course of CCl_4 treatment (Fig. 4C). In keeping, expression of genes related to the Notch pathway (*Notch1, Notch2, Jagged1, Hey-1*), whose activation is required for biliary specification,[10] were concordantly expressed at higher levels after 6 weeks of CCl_4, but not at later time-points (Fig. 4D).

DR cells clonally expand and differentiate into hepatocytes with a proliferative advantage

Our observations of transient DR and of the progressive rise in the size of DR-derived hepatocyte clusters suggest that few or single biliary cells expand as DR and undergo hepatocyte differentiation followed by several rounds of cell division. To test this hypothesis, we used the OPN-Cre;Rosa26R^{Confetti} mice[29] in which tamoxifen injections result in stochastic expression of 1 of the 4 fluorescent proteins (nGFP, mCFP, RFP and YFP) encoded in the confetti allele in the OPN$^+$ biliary cells. In control uninjured livers, 15–20% of cholangiocytes of the bile ducts were labelled with 1 of the 4 fluorescent proteins (Fig. S12). After CCl_4, all cells in a given DR expressed the same fluorescent protein (Fig. 5A), and not a mosaicism of different fluorescent proteins or of tagged/untagged cells. This observation supports that DR emerges from clonal expansion of a single biliary cell.

Also, all DR-derived hepatocytes within a patch were found to express the same single fluorescent protein (Fig. 5B). No mosaicism with a different fluorescent protein or with unlabelled hepatocytes was found in these patches. The dimension of the patches was similar to the dimension of those observed when using the Rosa26R^{YFP} reporter mice (Fig. S12b).

As also shown earlier in the OPN-Cre;Rosa26R^{YFP} livers (Figs. 1–3), the number of tagged hepatocytes in patches is larger than the number of cells in the original DR, suggesting that

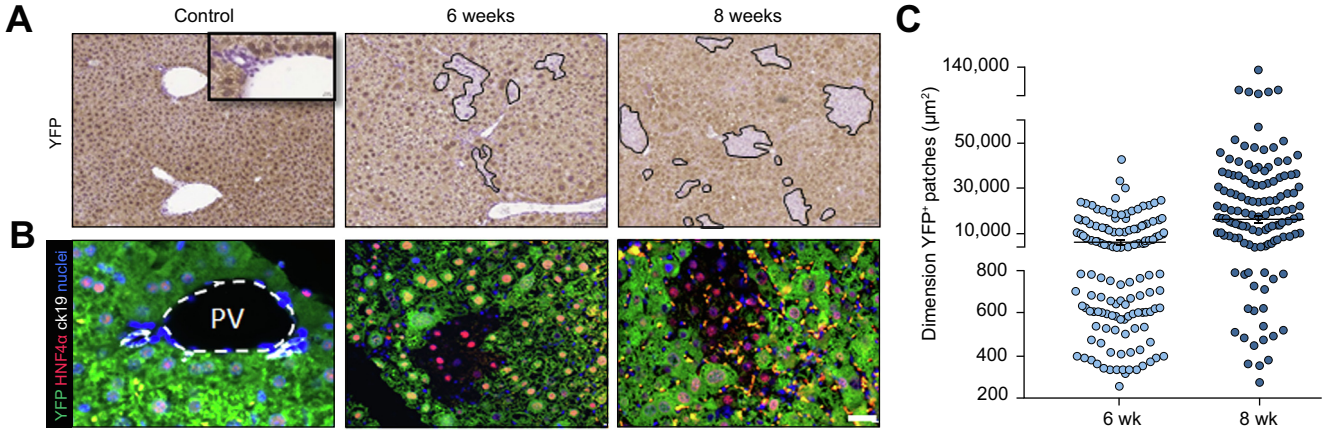

Fig. 3. Patches of new hepatocytes with no-hepatocytes origin. (A) Representative pictures of liver sections stained with YFP antibody in control mice (n = 5) and mice treated with CCl_4 for 6 (n = 4) and 8 (n = 4) weeks (scale bar: 100 µm). (B) Representative pictures of liver sections from AAV8-TBG-Cre;Rosa26R^{YFP} animals, CTLs and mice treated with CCl_4 for 6 and 8 weeks stained for HNF4α (red)/ YFP (green)/CK19 (white): in the CTL liver all the hepatocytes are YFP$^+$, expressed HNF4α but not CK19; in CCl_4 livers YFP$^+$ and YFP$^-$ hepatocytes were HNF4α+ CK19- (scale bar: 50 µm). (C) Size of the YFP- patches from the liver sections of AAV8-TBG-Cre;Rosa26R^{YFP} mice treated with CCl_4 for 6 and 8 weeks. CCl_4, carbon tetrachloride; CTL, control; PV, portal vein; YFP, yellow fluorescence protein.

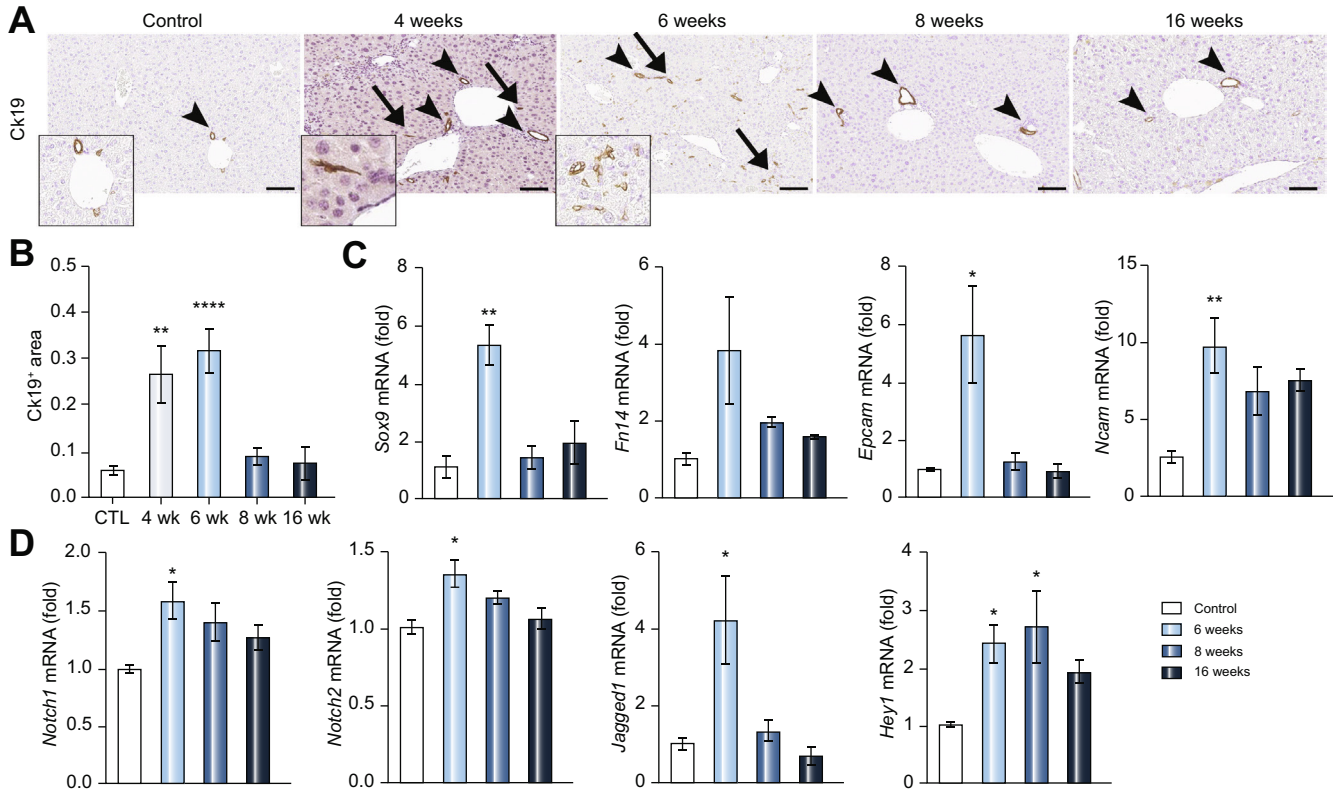

Fig. 4. Chronic CCl_4 results in progressive fibrosis and discrete transient DR. (A) Liver section obtained from OPN-iCreER^{T2};Rosa26R^{YFP} mice treated for 0 (n = 6), 4 (n = 2), 6 (n = 5), 8 (n = 4) and 16 (n = 4) weeks with CCl_4, stained with CK19 for bile ducts (arrowhead) and DR (black arrows). (Scale bars: 100 μm). Insert: higher magnifications of normal bile ducts and DR are shown. (B) Morphometrical quantification of CK19$^+$ cells confirms discrete and transient DR during the progression of the injury. (C) DR markers and (D) genes of the Notch pathway were determined by RT-qPCR. Values are expressed as mean ± SEM relatively to controls. *p <0.05; **p <0.01; ****p <0.0001 by 1-way ANOVA. CCl_4, carbon tetrachloride; CTL, control; DR, ductular reaction; RT-qPCR, reverse transcription quantitative PCR.

during chronic liver injury biliary cells undergo clonal proliferation before transforming into hepatocytes; the number of which subsequently increases due to several rounds of cell division.

If clonal expansion of differentiated hepatocytes support patch growth, we should observe transition features between DR cells and hepatocytes in nascent patches, but not at later stages. Thus, we measured the size of hepatocytes. Coherently, we found that DR-derived cells were significantly smaller than adjacent native hepatocytes at the early 6-week time-point, but at 16 weeks they were as large as native hepatocytes (Fig. 5C). The size of hepatocytes was also measured in the AAV8-TBG-Cre X Rosa26R^{YFP} mice, confirming the increase in size of unlabelled (non-hepatocyte origin) cells with the progression of the injury (Fig. S10B). DR-derived hepatocytes had a higher proliferation index (% of Ki67$^+$ cells) (Fig. 5D), a higher percentage of cells expressing cyclin D1 (Fig. S13) or engaged in mitosis (phosphohistone-H3 positive) (Fig. 5E) compared with native hepatocytes, further indicating that proliferation of differentiated mature cells contribute to growth of DR-derived hepatocytes patches

DR-derived hepatocytes respond better to stress signals

YFP$^+$ hepatocytes when located in the pericentral area (representing 10% of the YFP$^+$ hepatocytes contingent – [Fig. S8]) express CYP2E1 (Fig. 2C). Moreover, CYP2E1 and GS were similarly expressed at the same level in the DR-derived and native hepatocyte populations (Fig. S8D). We therefore assumed that a similar proportion of the 2 cell populations are able to metabolize CCl_4 and undergo CCl_4-induced damage. To study the cells' response to DNA damage, we checked the expression of genes involved in the DNA repair machinery in native (mTomato-Red) and DR-derived (mGFP-Green) injured hepatocytes, sorted after 6 and 8 weeks of CCl_4, and compared them with healthy control hepatocytes. The expression of *Brca1, Rad511* and *Fanci* (encoding for proteins that bind DNA damage site), expression of the gatekeeper *Gadd45* as well as of the checkpoint kinases 1 and 2 (*Chek1/2*) were similarly increased in the 2 populations of native and DR-derived injured hepatocytes compared to the healthy control hepatocytes (Fig. 6A). Moreover, upon CCl_4 exposure, a similar proportion of cells of the YFP$^+$ and YFP$^-$ population harbour nuclear γH2AX, a protein that aggregates to DNA breaks (Fig. 6B). The proportion of TUNEL$^+$ apoptotic cells was however lower in DR-derived than in native hepatocyte populations (Fig. 6C). Consistently, analysis from RNAseq data confirmed that the native population was enriched in the pathways involved in the regulation of DNA damage, apoptotic process and senescence (Fig. 6D).

Polyploidy, a feature of mature hepatocytes,[38] is determined by the number of nuclei per cell (cellular polyploidy) and the DNA content for each nucleus (nuclear polyploidy). During liver development, polyploidization is mostly associated with modification of cellular polyploidy[39] whereas under stress condition nuclear polyploidy is altered.[40] Thus, in the context of CCl_4 treatment, we have focused on nuclear polyploidy analysis. Compared to untreated controls, YFP$^-$ native hepatocytes dis-

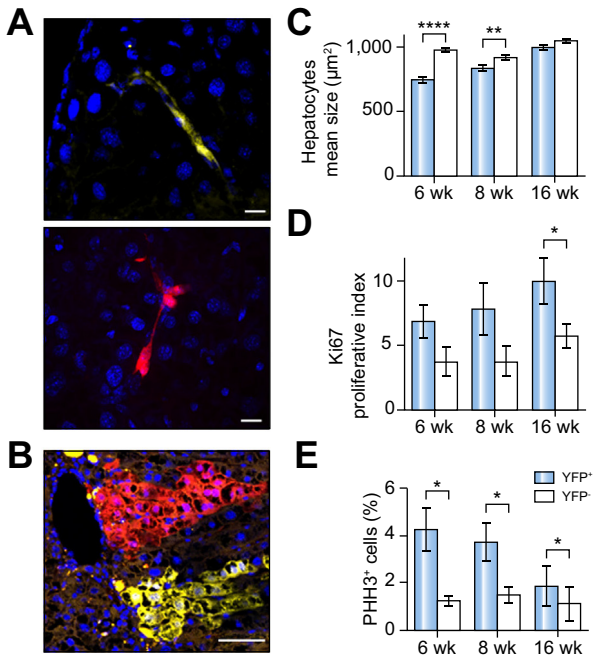

Fig. 5. Biliary cells in DR and DR-derived hepatocytes undergo clonal expansion. Representative confocal pictures of liver sections of OPN-iCreER^{T2};Rosa26R^{Confetti} mice treated with CCl_4 for 8 weeks (n = 4) showing (A) DR and (B) and DR-derived hepatocyte patches (scale bar: 20 µm). (C) Size in µm^2 (mean ± SEM) of YFP$^+$ and YFP$^-$ hepatocytes in OPN-iCreER^{T2};Rosa26R^{YFP} mice. Quantification of (D) ki67$^+$ and (E) phosphoHistone-H3 (PHH3)$^+$ hepatocytes in YFP$^+$ and YFP$^-$ populations in livers from OPN-iCreER^{T2};Rosa26R-YFP mice treated for 6 (n = 5), 8 (n = 4) and 16 (n = 4) weeks. $^*p$ <0.05 $^{**}p$ <0.01 **** p <0.001 by t test in (C–E). CCl_4, carbon tetrachloride; DR, ductular reaction; YFP, yellow fluorescence protein.

play a lower proportion of tetraploid nuclei (4 n), and a higher proportion of highly polyploid nuclei (≥8 n) as expected under CCl_4 stress conditions. By contrast, YFP$^+$ nuclei showed a similar polyploidy profile as untreated livers with a low proportion of highly polyploid nuclei (≥8 n) (Fig. 6E and Fig. S14). All these results suggest that although native and DR-derived hepatocytes similarly experience DNA damage in ongoing CCl_4-injury, DR-derived hepatocytes have a survival advantage over native hepatocytes with less cells driven into death or senescence.

DR-derived hepatocytes have a proliferative and DNA repair advantage upon recovery

Thus, newly formed DR-derived hepatocytes have less stress stigmata (and are potentially genetically more stable) and the balance proliferation/death favors their amplification over native hepatocytes. To verify the repopulation advantage of YFP$^+$ DR-derived cells, we exposed the mice to 16 weeks of CCl_4 and allowed the liver to recover for 2 or 4 weeks. The parenchymal area occupied by YFP$^+$ hepatocytes increased from 4.5% after 16 weeks of CCl_4 to 7.5% and up to 13.5% after 2 and 4 weeks recovery, respectively (Fig. 7A-B). The increase in the number of YFP$^+$ hepatocytes was explained by an increase in the size of YFP$^+$ clusters (Fig. 7C) and not by the number of clusters (not shown) or the cellular size (Fig. 7D). Although the total number of Ki67$^+$ cells decreased during recovery (Fig. S15), the proliferative index (Fig. 7E,F) and the number of pHH3$^+$ mitotic cells (Fig. 7G) was higher in YFP$^+$ than in YFP$^-$ hepatocytes upon recovery. γ-H2AX accumulates to form foci on damaged DNA to recruit DNA repair by homologous recombination upon injury. Indeed, as mentioned (Fig. 6B) and as shown in Fig. 7H, the 2 populations of hepatocytes upon injury similarly accumulated nuclear γH2AX. Persistence of nuclear γH2AX foci once injury has resolved indicate the presence of unrepaired DNA.[41] Native hepatocyte retained nuclear γH2AX protein upon recovery while it was rapidly cleaned in YFP$^+$ hepatocytes (Fig. 7H and Fig. S16). Collectively, these data support the concept that the increased number of DR-derived hepatocytes upon recovery from injury is achieved by effective proliferation of unstressed cells previously differentiated from DR, while YFP$^-$ native hepatocytes harbor unrepaired DNA damage and are significantly less replicative.

DR-derived hepatocytes are not involved in the development of preneoplastic nodules

The cirrhotic liver is a precancerous organ. Twenty-four weeks of CCl_4 caused macronodular cirrhosis (Fig. 8A-B). Although YFP staining revealed some cirrhotic nodules entirely composed by YFP$^+$ cells or mosaic YFP$^+$/YFP$^-$ (arrows in Fig. 6B), the majority of nodules were nonetheless YFP$^-$ (Fig. 8C). GS expression, a proxy for β-catenin activation described in preneoplastic lesions and a useful marker to identify neoplasia,[42] was found in 40% of YFP$^-$ nodules and only in 10% of YFP$^+$ regenerative nodules (Fig. 8D-E). Moreover, in mosaic YFP$^+$/YFP$^-$ nodules, GS expression was restricted to YFP$^-$ areas while YFP$^+$ DR-derived hepatocytes did not express GS (insert Fig. 8D). Compared to normal hepatocytes in the undamaged liver, YFP$^-$ native hepatocyte nuclei were more often highly polyploid (>8 n) and more rarely tetraploid (4 n) in the cirrhotic liver (Fig. 8F). By contrast, the level of nuclear polyploidy of DR-derived YFP$^+$ hepatocytes in the cirrhotic liver was comparable to that of hepatocytes in an undamaged liver (Fig. 8F) suggesting, also at this stage of the disease, a higher protection or a better capacity of DR-derived YFP$^+$ cells to manage stress induced by CCl_4 treatment. Similar to Tummala *et al.*[43] we applied to regenerative nodules a composite index based on immunodetection of GS, β-catenin and Ki67 (IHC score) for diagnosis of malignant hepatocellular neoplasms. The index was low in all cirrhotic nodules compared to scores in proven HCC[31] taken as reference (Fig. S17D), but notably the YFP$^+$ nodules had a lower score than the YFP$^-$ nodules (Fig. 8G). Then, we interrogated the susceptibility of native and DR-derived hepatocytes to carcinogenesis, using the carcinogenic agent diethylnitrosamine (Fig. S17A). Out of 15 mice, 12 developed macroscopic tumors. Altogether, 26 nodules were diagnosed as HCC (Fig. S17). They were, however, all YFP$^-$ and no YFP$^+$ HCC were found (Fig. S17).

Discussion

Recent studies have established that cells from the biliary compartment give rise to the DR and to functional hepatocytes.[15,24,26] The latter has been demonstrated in models in which hepatocellular injury associates with genetic abrogation of their replicative capacity[15,24,25] as well as in long-term TAA-injury model.[26] However, the kinetics of cell differentiation from a biliary precursor and characterization of the new hepatocytes have not been investigated to date.

The present study was designed to test the efficiency and safety of this alternative regeneration pathway in a model of chronic hepatocellular disease. We used a model of repeated administration of the hepatotoxic CCl_4 to induce repeated

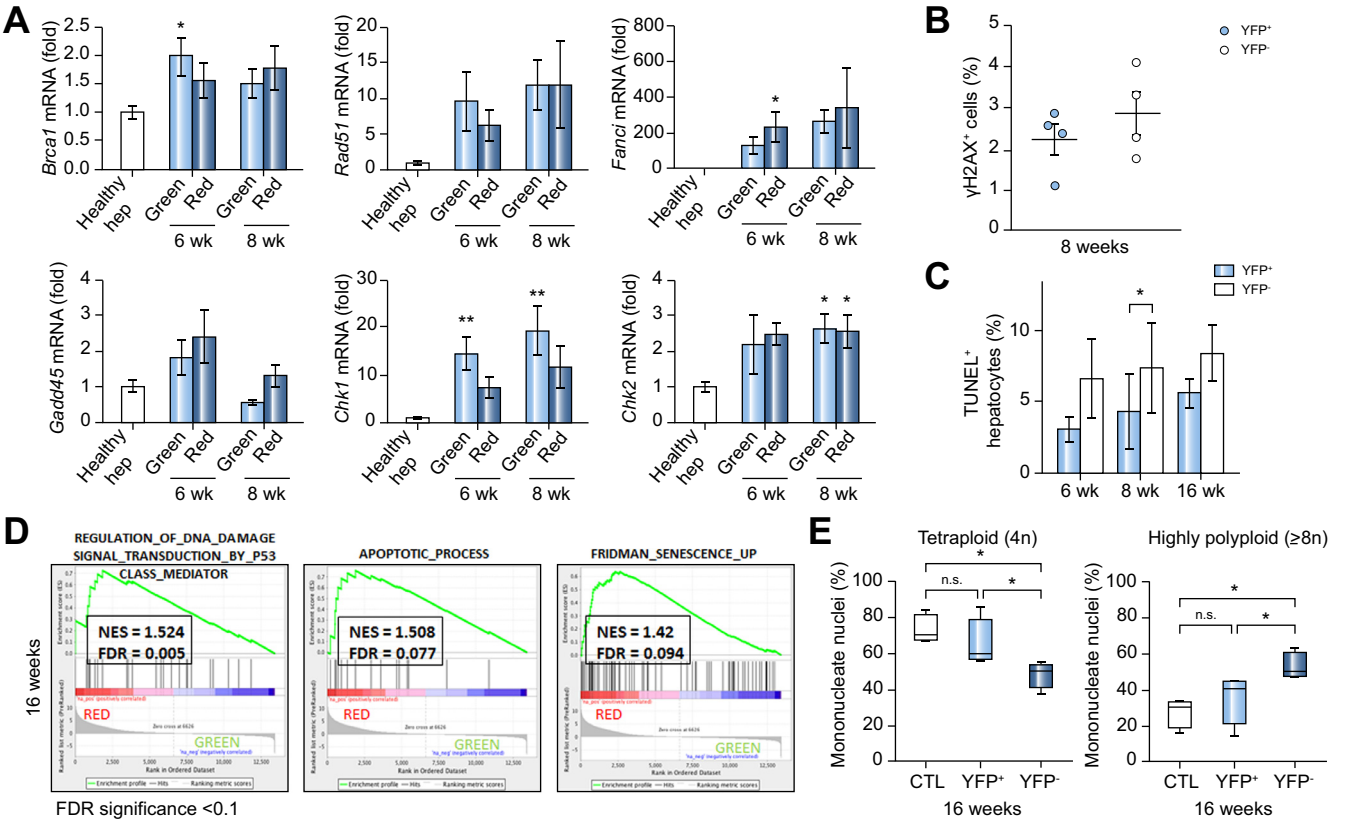

Fig. 6. Upon injury, DR-derived hepatocytes face the same DNA-damage level, but cope with it better. (A) Gene expression for genes involved in the DNA repair machinery in healthy hepatocytes (white bar), DR-derived hepatocytes (mGFP positive; light blue bar) and native hepatocytes (mTomato positive; dark blue bar) sorted from tamoxifen-treated OPN-iCreER^{T2};Rosa26R$^{mT/mG}$ mouse livers after 6 (n = 4) and 8 (n = 4) weeks CCl_4. Quantification of (B) γH2AX$^+$/YFP$^+$ and γH2AX$^+$/YFP$^-$ hepatocytes after 8 weeks CCl_4 (C) apoptotic TUNEL$^+$ hepatocytes in YFP$^+$ and YFP$^-$ populations in livers from OPN-iCreER^{T2};Rosa26R-YFP mice treated for 6, 8 and 16 weeks with CCl_4. (D) Gene Set enrichment analysis in mTomato (red) native hepatocytes and mGFP (green) DR-derived hepatocytes sorted from tamoxifen-treated OPN-iCreER^{T2};Rosa26R$^{mT/mG}$ mouse livers after 16 weeks of CCl_4 (E) Analysis of nuclear ploidy in OPN-iCreER^{T2};Rosa26R^{YFP} mice treated for 16 weeks with CCl_4 (n = 4). Box plot of the percentage of the tetraploid (4 n) and highly polyploid (≥8 n) nuclei relative to mononuclear polyploid nuclei. $^*p$ <0.05; $^{**}p$ <0.01 by *t* test in Mann-Whitney *U* test. CCl_4, carbon tetrachloride; DR, ductular reaction; GFP, green fluorescence protein; YFP, yellow fluorescence protein.

rounds of parenchymal necrosis and healing that culminate in cirrhosis, mimicking the evolution and severity of chronic liver injury in humans. The use of efficient and clean genetic tracing of cholangiocytes,[33] or conversely of native hepatocytes, enabled us to monitor the relationship between the DR and the generation of hepatocytes from the DR cell compartment, or from the hepatocyte pool, at various stages of disease progression. With these tools, our experiments demonstrate that ~12% of hepatocytes in the chronically ill liver derive from DR differentiation and not from replication of native pre-injury hepatocytes. In other studies,[14,30,44] including previous work from our lab,[13] DR cells were not found to contribute to liver regeneration in short term CCl_4-induced injury. The discrepancy results from the experimental protocol and whether it impedes hepatocyte regeneration. We followed the scheme already published by our lab: 3 injections of CCl_4 per week with adaptation of the dose to the body weight. 4 weeks of CCl_4, in the current work as in Español-Suner *et al.*[13] caused a discrete DR and no DR-derived hepatocytes were observed. In the others papers in which the expression "chronic CCl_4" was used, CCl_4 was administrated only twice a week, for 5, 6 or 8 weeks.[14,30,44] None of those papers reported the hepatocyte proliferation, but we can speculate that the dose and timing of the CCl_4 injections were not enough to inhibit hepatocyte proliferation. As evidence for this hypothesis, Pu *et al.* reported that the peripor-

tal Mfsd2a$^+$ native hepatocytes repopulate the liver lobules during "chronic" CCl_4, confirming that they are not in a state of replicative senescence.[34]

Similar to our data, Deng *et al.* recently published the contribution of cholangiocytes to parenchymal regeneration in a model of long lasting TAA-induced liver disease.[26] However, in the TAA model both native and cholangiocyte-derived hepatocytes had similar proliferation, as assessed by Ki67 analysis, leaving the mechanism for the rising proportion of cholangiocyte-derived hepatocytes at this time unexplained. Consistent with our data, the same authors reported using the AAV8-TBG-Cre;mTmG system, showing that after long-term (24 weeks) TAA insult, mTom$^+$ hepatocytes composed 20% of the parenchyma, *i.e.* 20% of the hepatocytes did not derive from proliferation of native mGFP$^+$ (and mTom$^-$) hepatocytes. In the same model, 7% of the hepatocytes were demonstrated to be of biliary origin. The difference in number might be ascribed to the relatively poor efficiency of biliary labelling in CK19-CreER mice (70%). By using a similar approach but a much more efficient system to trace biliary cells (>85% efficiency), the patches of hepatocytes that appear after long-term CCl_4 in our study were similar in size, whether traced as of DR-origin or, in the mirror experiment, as of non-hepatocytic origin.

In addition, we studied the temporal evolution of the DR differentiation process and found that, in CCl_4-induced injury,

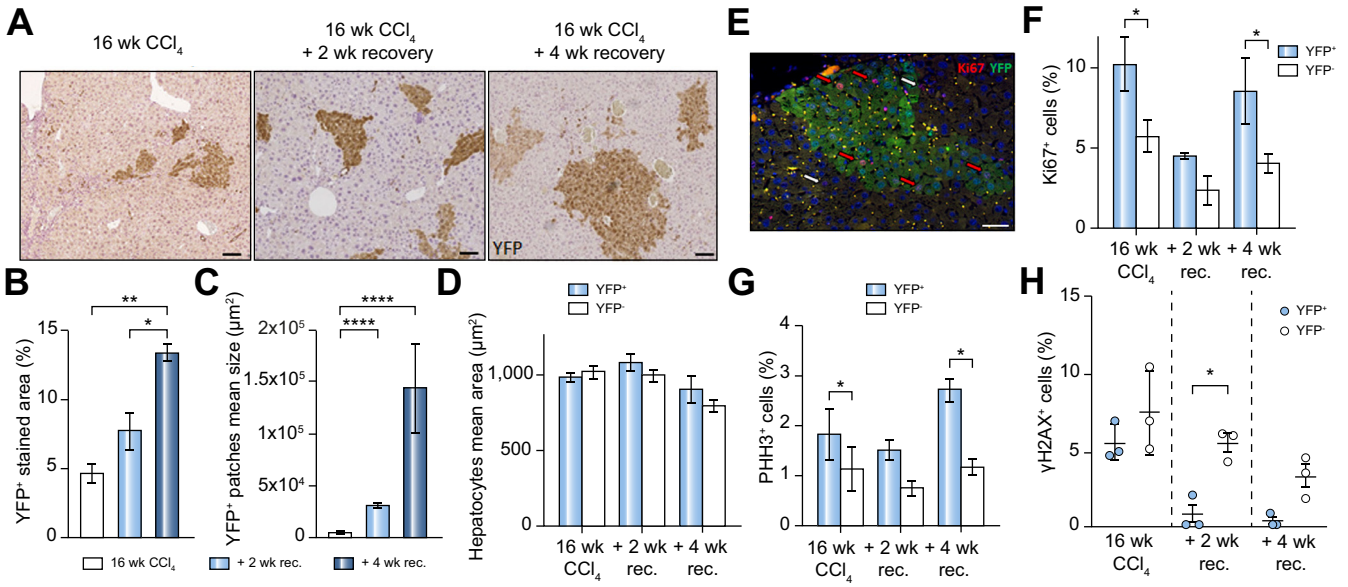

Fig. 7. DR-derived hepatocytes have a survival, proliferative and DNA repair advantage upon recovery. OPN-iCreER^{T2};Rosa26R^{YFP} mice were treated for 16 weeks with CCl_4 and analyzed 72 h after last CCl_4 injection (n = 4) or after 2 and 4 weeks of CCl_4-free recovery period (n = 4 and n = 3, respectively). (A) YFP immunohistochemistry (scale bar: 100 μm) with (B) morphometric quantification of YFP$^+$ area; (C) analysis of the size in the YFP$^+$ patches and (D) of the size (in μm^2) of the YFP$^+$ and YFP$^-$ hepatocytes. (E) Representative picture of liver sections stained for Ki67/YFP. Red arrows indicate the YFP$^+$ Ki67$^+$ DR-derived hepatocytes. On the contrary, the white arrows point to the YFP$^-$Ki67$^+$native hepatocytes (Scale bar: 50 μm). Quantification of the (F) Ki67 index and (G) PHH3 index in YFP$^+$ and YFP$^-$ hepatocytes; (H) Quantification of the γH2AX$^+$/YFP$^+$ and γH2AX$^+$/YFP$^-$ hepatocytes. $^*p$ <0.05, $^{**}p$ <0.01, $^{****}p$ <0.0001 by 1-way ANOVA (B,C,E) or *t* test (D,G,H). CCl_4, carbon tetrachloride; DR, ductular reaction; YFP, yellow fluorescence protein.

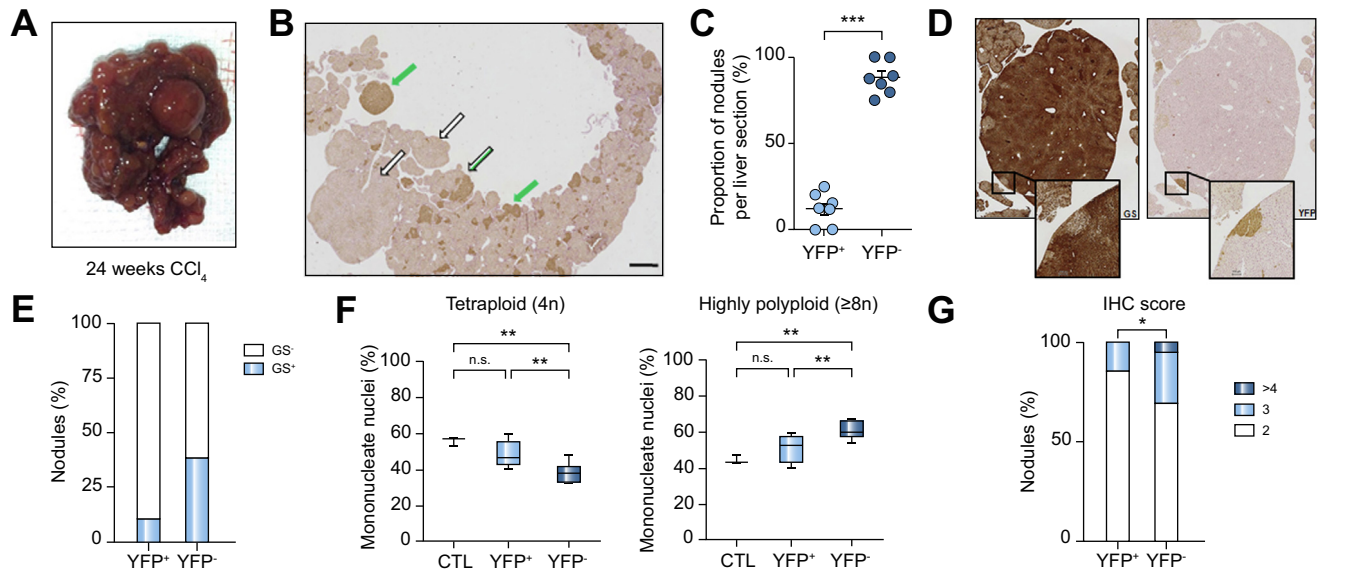

Fig. 8. DR-derived hepatocytes in cirrhotic regenerative nodules. (A) Representative liver harvested from OPN-iCreER^{T2};Rosa26R^{YFP} mice treated for 24 weeks with CCl_4 (n = 10), (B) YFP immunohistochemistry (bar size: 1 mm) with white arrows pointing towards YFP$^-$ nodules, green arrows towards YFP$^+$ nodules, and the white/green arrow towards a mosaic nodule. (C) Percentage of YFP$^+$ and YFP$^-$ nodules per liver section (one dot per liver). (D) Representative pictures of GS and YFP immunostaining on consecutive slides. (E) Analysis of GS expression in YFP$^+$ and YFP$^-$ regenerative nodules and (F) analysis of tetraploid (4 n) and highly polyploid (≥8 n) nuclei relative to mononuclear polyploid nuclei. (n = 3 in CTL group; n = 10 in CCl_4 group). (G) Immunohistochemistry score based on GS, β-catenin and Ki67 (see materials and methods) on YFP$^+$ and YFP$^-$ nodules. $^{***}p$ <0.001 by t test (c) $^{**}p$ <0.01 by Mann-Whitney *U* test (F) and $^*p$ <0.05 by Kolmogorov-Smirnov test (G). CCl_4, carbon tetrachloride; CTL, control; DR, ductular reaction; YFP, yellow fluorescence protein.

DR stems from clonal amplification of a discrete population of biliary cells, the identity of which remain to be ascertained. Thereafter DR cells, or a subset of them undergo complete hepatocytic differentiation yielding functional cells, perfectly organized within the lobular architecture (Fig. 3). Consistent with studies by Lu *et al.*[16] and Raven *et al.*[24] initial differentiation of DR cells into hepatocytes coincided with the injury-induced drop in replication of native hepatocytes and their entry into senescence as supported by P21 expression, senescence-associated β-galactosidase activity and expression of the senescence-associated gene program (SASP).

Morphometric analyses revealed that early in the process, newly differentiated hepatocytes are small in size and reach a normal size with time while they amplify. Clonality experiments in confetti mice highlight that all DR-derived hepatocytes within a patch harbor 1 unique fluorescent tag, identical to that expressed by adjacent DR cells, signaling their genetic filiation. Yet when hepatocyte patches expand, DR vanishes. These data suggest that during chronic liver injury, DR does not constantly re-fuel the parenchyma with newly differentiated cells, but rather when sufficient and appropriate cellular and environmental conditions are met, a limited contingent of DR cells undergo differentiation then clonal expansion to repopulate up to 12% of the liver. Further studies will be needed to determine whether the subset of DR cells that are capable of yielding hepatocytes could correspond to $ST14^{hi}$ clonogenic cholangiocytes,[45] or $Lgr5^{+}$ liver stem cells[46], or the peripheral ductule described by Kamimoto *et al.*[6]. Pulse labelling of DR cells during disease progression would be required to test this hypothesis.[6]

Our experimental system also permits the separate analysis of the properties and contribution to regeneration of newly generated hepatocytes and native hepatocytes, *i.e.* those already present before injury. At all times in the process, proliferative and mitotic indices are higher in the newly emerged population of hepatocytes than in native hepatocytes. Cell death by apoptosis and senescence are conversely readily seen in native hepatocytes during chronic exposure to CCl_4 but not in adjacent DR-derived hepatocytes, supporting a proliferative advantage of the latter over native hepatocytes. These findings suggest an explanation for sometimes extensive parenchymal reconstitution in advanced-stage chronic viral hepatitis in humans[9] that has not been convincingly demonstrated in acute or mild human hepatic injury or in most animal models of human disease. As native hepatocytes eventually become damaged and consequently senescent, the DR-derived hepatocytes then begin to repopulate because of their untapped replicative potential.[9] This proposal was further supported by a higher proliferation rate of the DR-derived population once the injurious toxin was retrieved, resulting in a significant proportional increase in the lobular area occupied by DR-derived hepatocytes and hence a decreased proportion of native hepatocytes in the lobules. As a result, DR contributed to the regeneration of a significant proportion of the parenchyma in the chronically injured liver.

The ploidy pattern of DR-derived and native hepatocytes also differed. As reported elsewhere[40] various stress signals, including oxidative stress, provoke a decrease in the proportion of stable tetraploid nuclei and a rise in that of highly polyploid nuclei. In a context of CCl_4 treatment, we observed this precise stress-induced shift in native hepatocytes but not in DR-derived hepatocytes. Indeed, the latter, although being exposed to CCl_4 and appropriately expressing CYP2E1 necessary for CCl_4 activation, exhibited a nuclear polyploid pattern similar to that of liver parenchymal cells in an unarmed liver. This differential ploidy pattern persisted despite continuation of CCl_4 administration. By maintaining a less polyploid genome, DR-derived hepatocytes would, like stem cells do, retain a higher replicative potential with a lower risk of accumulating DNA damage. In support to this, DR-derived hepatocytes in the healing liver retained less γH2AX foci and thus unrepaired DNA. Moreover, when exposed to DEN, a carcinogenic agent, native but not DR-derived hepatocytes underwent carcinogenic transformation, highlighting the stress resistance and stability of the latter. Whether indeed DR-driven regeneration reduces the risk of cancer would need to be confirmed in dedicated studies.

Herein, we have provided evidence that a population of younger and healthier hepatocytes traced from cholangiocytes and not from hepatocytes emerges in an injured liver. Therefore, stimulation of DR-derived regeneration *in vivo* appears to be a safe strategy to alleviate liver insufficiency in chronic liver disease. However, several key issues are awaiting answers. Our experimental design does not allow for identification of the characteristics that enable (a subset of) biliary cells with reactive capacity to mount the DR (the "target cells" for DR-derived regeneration). They could correspond to the label retaining cells recently described by Cao *et al.*[47] Also, while failure of mature hepatocytes to divide and regenerate the organ contributes to trigger DR and its differentiation, many other processes activated during wound repair are likely to be involved, such as vascular changes, inflammation, modification of the extracellular matrix scaffold, *etc.*[8,12,48] Whether all small DR-derived hepatocytes undergo clonal expansion and equally contribute to liver regeneration is not answered by the present study. We observed, when liver disease becomes severe and while the number of DR-derived hepatocytes increases in growing foci, a decline in the total amount of YFP^{+} cells owing to a drop in the number of small foci. The absence of mosaicism in DR-derived hepatocyte foci in confetti mice does not support a confluence of growing foci. Therefore, we suppose that a large proportion of emerging small DR-hepatocytes do not survive in a stressed organ or are not similarly exposed to, or do not similarly respond to, stimuli to enable complete differentiation and proliferation. A better understanding of the mechanisms supporting DR-derived regeneration is now the next research goal, in order to identify pathways amenable to therapeutic manipulation for the treatment of liver insufficiency.

Financial support

This work was supported by grants from the Belgian Federal Science Policy Office (Interuniversity Attraction Poles program, network P7/83-HEPRO2 and from the Fund for Scientific Medical Research (FNRS-PDR T.1067.14-P) to IA.L. and from unrestricted from Gilead, Belgium.

Conflict of interest

The authors declare no competing personal or financial interests.

Please refer to the accompanying ICMJE disclosure forms for further details.

Authors' contributions

R.M. designed, conducted the experiments, analyzed and discussed the data, L-A.C. analyzed and discussed the data, S.V. and LA. vG. generated, analyzed and discussed the FACS analysis, analyzed and discussed the RNAseq data, M.B-N. and C.D. generated, analyzed and discussed the ploidy data, C.S. generated the HIC score and discussed the data, J.A., B.B. and J.L. Gala analyzed and discussed the RNAseq data, Y.H. discussed the hypothesis, study design and data, I.L. designed the experiments, conducted the study, and analyzed and discussed the

data; R.M. and I.L. wrote the original manuscript. All authors read and edited the manuscript.

Acknowledgement

Rosa26R-Confetti reporter mice were a kind gift of Prof. Cedric Blanpain (Université Libre de Bruxelles (ULB), Belgium). Rosa26-mTmG mice were a kind gift of Prof. Holger Gerhardt (KULeuven, Belgium). The authors thank Prof. F. Lemaigre (DDve Institute, UCL, Brussels, Belgium), who generated the OPN-iCreER^{T2} mice and made them available for our studies; N. Feza-Bingi and V. Lebrun (GAEN lab, UCL, Brussels, Belgium) for excellent technical and animal support; D. Brusa from IREC FACS platform and N. Dauguet from De Duve Institute – Flow cytometry and cell sorting platform in Université Catholique de Louvain for excellent technical assistance; D. Tyteca and P. Van Der Smissen (De Duve Institute, UCLouvain, Brussels, Belgium) for assistance with confocal microscopy and Dr E. Danse (Radiology department, St Luc University hospital and UCLouvain, Brussels Belgium) who performed ultrasound examination of the mice; Prof. G. Farrell for discussion and critical comments on the manuscript.

Supplementary data

Supplementary data to this article can be found online at https://doi.org/10.1016/j.jhep.2019.02.003.

References

Author names in bold designate shared co-first authorship

[1] Byass P. The global burden of liver disease: a challenge for methods and for public health. BMC Med 2014;12:159. https://doi.org/10.1186/s12916-014-0159-5.
[2] European Association for the Study of the Liver. Hepamap: a Roadmap for Hepatology Research in Europe: an Overview for Policy Makers 2017.
[3] Roskams T. Progenitor cell involvement in cirrhotic human liver diseases: From controversy to consensus. J Hepatol 2003;39:431–434.
[4] Van Hul NKM, Abarca-Quinones J, Sempoux C, Horsmans Y, Leclercq IA. Relation between liver progenitor cell expansion and extracellular matrix deposition in a CDE-induced murine model of chronic liver injury. Hepatology 2009;49:1625–1635.
[5] **Roskams TA**, **Theise ND**, Balabaud C, Bhagat G, Bhathal PS, Bioulac-sage P, et al. Nomenclature of the finer branches of the biliary. Hepatology 2004;39:1739–1745. https://doi.org/10.1002/hep.20130.
[6] Kamimoto K, Kaneko K, Kok CYY, Okada H, Miyajima A, Itoh T. Heterogeneity and stochastic growth regulation of biliary epithelial cells dictate dynamic epithelial tissue remodeling. eLife 2016;5:1–26.
[7] Roskams TA, Libbrecht L, Desmet VJ. Progenitor cells in diseased human liver. Semin Liver Dis 2003;23:385–396. https://doi.org/10.1055/s-2004-815564.
[8] Stueck AE, Wanless IR. Hepatocyte buds derived from progenitor cells repopulate regions of parenchymal extinction in human cirrhosis. Hepatology 2015;61:1696–1707. https://doi.org/10.1002/hep.27706.
[9] **Yoon S**, **Gerasimidou D**, Kuwahara R, Hytiroglou P, Yoo JE, Park YN, et al. Epithelial cell adhesion molecule (EpCAM) marks hepatocytes newly derived from stem/progenitor cells in humans. Hepatology 2010;53:964–973. https://doi.org/10.1002/hep.24122.
[10] Boulter L, Govaere O, Bird TG, Radulescu S, Ramachandran P, Pellicoro A, et al. Macrophage-derived Wnt opposes Notch signaling to specify hepatic progenitor cell fate in chronic liver disease. Nat Med 2012;18:572–579. https://doi.org/10.1038/nm.2667.
[11] Gouw ASH, Clouston AD, Theise ND. Ductular reactions in human liver: Diversity at the interface. Hepatology 2011;54:1853–1863. https://doi.org/10.1002/hep.24613.
[12] **Falkowski O**, **An HJ**, Ianus IA, Chiriboga L, Yee H, West AB, et al. Regeneration of hepatocyte "buds" in cirrhosis from intrabiliary stem cells. J Hepatol 2003;39:357–364. https://doi.org/10.1016/S0168-8278(03)00309-X.
[13] Español-Suñer R, Carpentier R, Van Hul N, Legry V, Achouri Y, Cordi S, et al. Liver progenitor cells yield functional hepatocytes in response to chronic liver injury in mice 1564–75.e7. Gastroenterology 2012;143. https://doi.org/10.1053/j.gastro.2012.08.024.
[14] Rodrigo-Torres D, Affo' S, Coll M, Morales-Ibanez O, Millàn C, Blaya D, et al. The biliary epithelium gives rise to liver progenitor cells. Hepatology 2014;60:1367–1377.
[15] Jörs S, Jeliazkova P, Ringelhan M, Thalhammer J, Dürl S, Ferrer J, et al. Lineage fate of ductular reactions in liver injury and carcinogenesis. J Clin Invest 2015;125:2445–2457. https://doi.org/10.1172/JCI78585.
[16] Lu W-Y, Bird TG, Boulter L, Tsuchiya A, Cole AM, Hay T, et al. Hepatic progenitor cells of biliary origin with liver repopulation capacity. Nat Cell Biol 2015;17:971–983.
[17] He J, Lu H, Zou Q, Luo L. Regeneration of liver after extreme hepatocyte loss occurs mainly via biliary transdifferentiation in zebrafish. Gastroenterology 2014;146(789–800). https://doi.org/10.1053/j.gastro.2013.11.045 e8.
[18] Malato Y, Naqvi S, Schürmann N, Ng R, Wang B, Zape J, et al. Fate tracing of mature hepatocytes in mouse liver homeostasis and regeneration. J Clin Invest 2011;121:4850–4860. https://doi.org/10.1172/JCI59261DS1.
[19] Schaub JR, Malato Y, Gormond C, Willenbring H. Evidence against a stem cell origin of new hepatocytes in a common mouse model of chronic liver injury. Cell Rep 2014;8:933–939. https://doi.org/10.1016/j.celrep.2014.07.003.
[20] Yanger K, Zong Y, Maggs LR, Shapira SN, Maddipati R, Aiello NM, et al. Robust cellular reprogramming occurs spontaneously during liver regeneration. Genes Dev 2013;27:719–724. https://doi.org/10.1101/gad.207803.112.
[21] Sekiya S, Suzuki A. Hepatocytes, rather than cholangiocytes, can be the major source of primitive ductules in the chronically injured mouse liver. Am J Pathol 2014;184:1468–1478. https://doi.org/10.1016/j.ajpath.2014.01.005.
[22] Tarlow BD, Pelz C, Naugler WE, Wakefield L, Wilson EM, Finegold MJ, et al. Bipotential adult liver progenitors are derived from chronically injured mature hepatocytes. Cell Stem Cell 2014;15:605–618. https://doi.org/10.1016/j.stem.2014.09.008.
[23] Clouston AD, Powell EE, Walsh MJ, Richardson MM, Demetris AJ, Jonsson JR. Fibrosis correlates with a ductular reaction in hepatitis C: roles of impaired replication, progenitor cells and steatosis. Hepatology 2005;41:809–818. https://doi.org/10.1002/hep.20650.
[24] **Raven A**, **Lu W**, Man TY, Ferreira-gonzalez S, Duibhir EO, Dwyer BJ, et al. Cholangiocytes act as facultative liver stem cells during impaired hepatocyte regeneration. Nature 2017;547:350–354. https://doi.org/10.1038/nature23015.
[25] Russell JO, Lu W-Y, Okabe H, Abrams M, Oertel M, Poddar M, et al. Hepatocyte-specific β-catenin deletion during severe liver injury provokes cholangiocytes to differentiate into hepatocytes. Hepatology 2018. https://doi.org/10.1002/hep.30270.
[26] Deng X, Zhang X, Li W, Feng RX, Li L, Yi GR, et al. Chronic liver injury induces conversion of biliary epithelial cells into hepatocytes 114–22.e3. Cell Stem Cell 2018;23. https://doi.org/10.1016/j.stem.2018.05.022.
[27] Srinivas S, Watanabe T, Lin CS, William CM, Tanabe Y, Jessell TM, et al. Cre reporter strains produced by targeted insertion of EYFP and ECFP into the ROSA26 locus. BMC Dev Biol 2001;1:4. https://doi.org/10.1186/1471-213X-1-4.
[28] Muzumdar MD, Tasic B, Miyamichi K, Li L, Luo L. A global double-fluorescent Cre reporter mouse. Genesis 2007;45:418–426. https://doi.org/10.1002/dvg.
[29] Livet J, Weissman TA, Kang H, Draft RW, Lu J, Bennis RA, et al. Transgenic strategies for combinatorial expression of fluorescent proteins in the nervous system. Nature 2007;450:56–62. https://doi.org/10.1038/nature06293.
[30] Tarlow BD, Finegold MJ, Grompe M. Clonal tracing of Sox9+ liver progenitors in mouse oval cell injury. Hepatology 2014;60:278–289. https://doi.org/10.1002/hep.27084.
[31] Mu X, Español-suñer R, Mederacke I, Affò S, Manco R, Sempoux C, et al. Hepatocellular carcinoma originates from hepatocytes and not from the progenitor/biliary compartment. J Clin Invest 2015;125:3891–3903. https://doi.org/10.1172/JCI77995DS1.
[32] Stradiot L, Verhulst S, Roosens T, Øie CI, Moya IM, Halder G, et al. Functionality based method for simultaneous isolation of rodent hepatic sinusoidal cells. Biomaterials 2017;139:91–101. https://doi.org/10.1016/j.biomaterials.2017.05.047.
[33] Ferreira-Gonzalez S, Lu WY, Raven A, Dwyer B, Man TY, O'Duibhir E, et al. Paracrine cellular senescence exacerbates biliary injury and impairs regeneration. Nat Commun 2018;9:1–15. https://doi.org/10.1038/s41467-018-03299-5.
[34] Pu W, Zhang H, Huang X, Tian X, He L, Wang Y, et al. Mfsd2a+hepatocytes repopulate the liver during injury and regeneration. Nat Commun 2016;7:1–15. https://doi.org/10.1038/ncomms13369.

[35] Antoniou A, Raynaud P, Cordi S, Zong Y, Tronche F, Jacquemin P, et al. Intrahepatic bile ducts develop according to a new mode of tubulogenesis regulated by the transcription factor SOX9. Gastroenterology 2010;136:2325–2333. https://doi.org/10.1053/j.gastro.2009.02.051. Intrahepatic.
[36] Jakubowski A, Ambrose C, Parr M, Lincecum JM, Wang MZ, Zheng TS, et al. TWEAK induces liver progenitor cell proliferation. J Clin Invest 2005;115:2330–2340. https://doi.org/10.1172/JCI23486.
[37] Roskams T, Van Haele M. Hepatic progenitor cells: an update. Clin Liv Dis 2010;46:409–420. https://doi.org/10.1016/j.gtc.2017.01.011.
[38] Gentric G, Desdouets C. Polyploidization in liver tissue. Am J Pathol 2014;184:322–331. https://doi.org/10.1016/j.ajpath.2013.06.035.
[39] **Hsu SH**, **Delgado ER**, Otero PA, Teng KY, Kutay H, Meehan KM, et al. MicroRNA-122 regulates polyploidization in the murine liver. Hepatology 2016;64:599–615. https://doi.org/10.1002/hep.28573.
[40] Gentric G, Maillet V, Paradis V, Couton D, L'Hermitte A, Panasyuk G, et al. Oxidative stress promotes pathologic polyploidization in nonalcoholic fatty liver disease. J Clin Invest 2015;125:981–992. https://doi.org/10.1172/JCI73957.
[41] Firsanov DV, Solovjeva LV, Svetlova MP. H2AX phosphorylation at the sites of DNA double-strand breaks in cultivated mammalian cells and tissues. Clin Epigenetics 2011;2:283–297. https://doi.org/10.1007/s13148-011-0044-4.
[42] Salleng KJ, Revetta FL, Deane NG, Washington MK. The applicability of a human immunohistochemical panel to mouse models of hepatocellular neoplasia. Comp Med 2015;65:398–408.
[43] Tummala KS, Brandt M, Teijeiro A, Graña O, Schwabe RF, Perna C, et al. Hepatocellular carcinomas originate predominantly from hepatocytes and benign lesions from hepatic progenitor cells. Cell Rep 2017;19:584–600. https://doi.org/10.1016/j.celrep.2017.03.059.
[44] Font-Burgada J, Shalapour S, Ramaswamy S, Hsueh B, Rossell D, Umemura A, et al. Hybrid periportal hepatocytes regenerate the injured liver without giving rise to cancer. Cell 2015;162:766–779. https://doi.org/10.1016/j.cell.2015.07.026.
[45] Li B, Dorrell C, Canaday PS, Pelz C, Haft A, Finegold M, et al. Adult mouse liver contains two distinct populations of cholangiocytes. Stem Cell Rep 2017;9:478–489. https://doi.org/10.1016/j.stemcr.2017.06.003.
[46] **Huch M**, **Dorrell C**, Boj SF, Van Es JH, Li VSW, Van De Wetering M, et al. In vitro expansion of single Lgr5 + liver stem cells induced by Wnt-driven regeneration. Nature 2013;494:247–250. https://doi.org/10.1038/nature11826.
[47] Cao W, Chen K, Bolkestein M, Yin Y, Verstegen MMA, Bijvelds MJC, et al. Dynamics of proliferative and quiescent stem cells in liver homeostasis and injury. Gastroenterology 2017;153:1133–1147. https://doi.org/10.1053/j.gastro.2017.07.006.
[48] Lin WR, Lim SN, McDonald SAC, Graham T, Wright VL, Peplow CL, et al. The histogenesis of regenerative nodules in human liver cirrhosis. Hepatology 2010;51:1017–1026. https://doi.org/10.1002/hep.23483.